Evaluation of tumor interstitial fluid-extraction methods for proteome analysis: comparison of biopsy elution versus centrifugation

Clara Matas-Nadal[1*], Joan Josep Bech-Serra[3], Marta Guasch-Vallés[1,2], Josep Manel Fernández-Armenteros[1,4], Carla Barceló[1], Josep Manel Casanova[1,4], Carolina de la Torre Gómez[3], Rafael Aguayo Ortiz[1,4§] and Eloi Garí[1§].

[1]Cell cycle lab. Institut de Recerca Biomèdica de Lleida (IRB Lleida). [2]Dept. Ciències Mèdiques Bàsiques. Facultat de Medicina. Universitat de Lleida. [3]Proteomics Unit, Josep Carreas Leukaemia Research Institute (IJC). [4]Servei de Dermatologia, Hospital Universitari Arnau de Vilanova, Lleida.

[§] RA and EG are co-senior authors.

*Corresponding Author: E-mail: clamanadal@gmail.com. Telephone number: 0034-680735376

ABSTRACT

The analysis of Tumor Interstitial Fluid (TIF) composition is a valuable procedure to identify anti-metastatic targets, and different laboratories have set up techniques for TIF isolation and proteomic analyses. However, those methods had never been compared in samples from the same tumor and patient. In this work, we compared the two most used methods, elution and centrifugation, in pieces of the same biopsy samples of cutaneous squamous cell carcinoma (cSCC). First, we established that high G-force (10000g) was required to obtain TIF from cSCC by centrifugation. Secondly, we compared the centrifugation method with the elution method in pieces of three different cSCC tumors. We found that the mean protein intensities based in the number of peptide spectrum matches was significantly higher in the centrifuged samples than in the eluted samples. Regarding the robustness of the methods, we observed higher overlapping between both methods (77-80%) than among samples (50%). These results suggest that exists an elevated consistence of TIF composition independently of the method used. However, we observed a three-fold increase of extracellular proteins in non-overlapped proteome obtained by centrifugation. We therefore conclude that centrifugation is the method of choice to study the proteome of TIF from cutaneous biopsies.

KEYWORDS: Tumor interstitial fluid, proteome, centrifugation, spin, elution, cutaneous squamous cell carcinoma, skin cancer

INTRODUCTION

Tumor-host interface signals are key elements to explain the induction and development of metastasis[1]. It seems clear that tumor-bearing extracellular signals are involved in most of metastatic steps such as stroma invasion and pre-metastatic niche preparation. This metastatic signaling is mediated by cancer-secreted metabolites and proteins. The secretome of a cell encompasses all the components secreted by this cell including metabolites, proteins and exosome vesicles. The cancerous secretome can be obtained from the tumor interstitial fluid (TIF). This fluid is bathing the tumor and stroma cells and represents the tumor milieu[2]. Therefore, the proteomic study of TIF is an approach of special interest that could reveal key molecules involved in the infiltrative or metastatic capacity of the neoplasia and could have potential consequences for developing biomarkers or therapeutic targets[3-4].

Proteomic analyses are well established methodologies for studies of molecular oncology[5]. However, these methods require a considerable effort to set up every step of the workflow in order to minimize pre-analytical and analytical variability. The main goal is to perform reproducible experiments and to obtain reliable lists of protein candidates. The initial step in the workflow is the sample preparation. Definitely, the quality of the starting material is a major prerequisite for the final-result quality. In addition, it is important to consider that sample preparation is not automated in most of the experiments[6]. Then, this step is one of the main sources of experimental variability[7].

Different techniques have been used for TIF isolation and proteomic analysis in different tumors[3]. It is because the choice of the right method for TIF isolation is not easy since it depends on many variables[8]. For instance, it is important to consider such diverse issues as the analytical purpose of the experiment, the amount of cell breakage or the volume recovered. Lacking a generally accepted method for TIF sampling, in this work, we have assayed the two most used methods of TIF isolation, elution and centrifugation, in the same biopsies of cutaneous squamous cell carcinoma (cSCC). This cancer is the second most common non-melanoma skin cancer and the second most common tumor in humans, and no proteomic study on its TIF has been conducted to date.

EXPERIMENTAL SECTION

Human cutaneous squamous cell carcinoma samples

The study was conducted following the basic principles (respect for the individual), operational (risk-benefit) and guidelines (good clinical practice) of the Declaration of Helsinki (World Medical Association, 1964). The samples came from diagnostic tissue

surplus and were collected after obtaining the written informed consent of the patient and with the approval of the Ethics Committee for Scientific Research (CEIC) of HUAV-UdL. The samples were managed by the Biobank of IRB Lleida authorized by the Department of Health of Catalonia dated 29 April 2013 and registered in the National Register of Biobanks of the Carlos III Institute of Health with B.0000682 reference number. The Biobank guarantees the conditions of traceability, quality and safety of the samples with the proper controls.

Three surplus biopsies of cSCC from patients were obtained after surgical resection and extensively washed with a sterile dressing to eliminate blood clots. The tumor samples were from the tumor surface, in an area without any apparent necrosis or inflammation. Immediately, the tissue was collected with sterile forceps and put on a plate (6-well) with 1 ml of PBS. The forceps was used to gently shake the tissue in the PBS and the washing was repeated three times. The tissue was cut into two equal halves in volume and tissue characteristics.

Elution method

For large biopsies (>0.2 gr), tissue was carefully cut into small pieces (0.1 gr) avoiding as long as possible cell damage with the minimum manipulation. The cutting of tissue was done while keeping it in a full of PBS plate, in order to avoid TIF evaporation. Then, eluted in 750 µl of PBS containing protease and phosphatase inhibitors (PBSi) for 2 hours at 37ºC and 5% CO_2. Finally, 500 µl of PBSi were collected and filtered (0.45 µm) to avoid cells contamination. The final sample was stored at -80ºC until the proteomic analysis. The cocktail of protease and phosphatase inhibitors (cOmplete™, EDTA-free Protease Inhibitor Cocktail) was purchased at Roche.

Centrifugation method

In this method, biopsy was blotted gently with tissue paper to remove excess of PBS and transferred to 2 ml centrifuge tubes (Clearspin 2 ml tubes. 0.45 mm Cellulose acetate membrane. Sterile ClearLine (Ref 007859ACL)) used for TIF isolation. These two steps were carried out quickly to avoid evaporation from the tissue. Immediately, the samples were centrifuged at 10000 g for 20 minutes at 4ºC (Eppendorf, 5415R), recovering 5-15 µl accumulated in the bottom of the tube. PBSi was added for a final volume of 50 µl. This final sample was stored at -80ºC until the proteomic analysis.

Electrophoresis

TIF proteins from each method were separated on a 10% SDS-PAGE gel. To visualize protein bands, the gel was stained with Coomassie Blue reagent. The protein profile of the samples was obtained with the plot profile of Image J program.

Proteomic analysis of the samples

Protein extraction, quantification and digestion

The TIFs were mixed with 6M Urea / 200mM Ammonium Bicarbonate (ABC) to help the proteins to be solubilized and then quantified with the RCDC Protein Assay kit (Biorad, #5000-120). Ten µg of protein from each sample were digested in-solution using both LysC and Trypsin. Briefly, the samples were reduced with 10mM dithiothreitol (DTT, in 200mM ABC) for 1h at 37ºC and 650 rpm in the thermo-mixer, alkylated with 20 mM iodoacetamide (IAA, in 200mM ABC) for 30 minutes at room temperature in the dark at 650 rpm in the thermo-mixer. Then, samples were diluted to have them at 2M Urea final concentration and the required amount of 1µg/µl LysC (WAKO, #125-05061) was added to have a 1:10 ratio enzyme:protein (w:w). The digestion was performed overnight at 37ºC at 650 rpm in the thermo-mixer. After that, samples were diluted again to have them at 1M Urea final concentration. Finally, the required amount of 1µg/µl trypsin (sequencing-grade, Promega, #V5280) was added to have a 1:10 ratio enzyme:protein (w:w) and incubated for 8h at 37ºC at 650 rpm in the thermo-mixer.

Peptide desalting

Peptide mixtures were desalted using the commercial columns Ultra Microspin C18, 300A silica (The Nest Group, #SUM SS18V) according to the manufacturer instructions. Finally, the samples were dried in a SpeedVac and kept at -20ºC until the LC-MS/MS analysis.

LC-MS/MS analysis

Samples were analyzed in a Proxeon 1000 liquid chromatographer coupled to an Orbitrap Fusion Lumos (Thermo Fisher Scientific) mass spectrometer. Samples were re-suspended in 45 microliters of 0.5% formic acid in water, and 4.5 µl (2 micrograms) were injected for LC-MSMS analysis. Peptides were trapped on an NTCC-360/75-3-123 LC column and separated using a C18 reverse phase LC column-Easy Spray (Thermo Fisher Scientific). The gradient used for the elution of the peptides was 1% to 35% in 90min followed by a gradient from 35% to 85% in 10 min with 250nL/min flow rate. Eluted peptides were subjected to electrospray ionization in an emitter needle (PicoTipTM, New

Objective, Scientific Instrument Services, Ringoes, NJ, USA) with an applied voltage of 2,000 V. Peptide masses (m/z 300-1700) were analyzed in data-dependent mode where a full scan MS was acquired on the Orbitrap with a resolution of 60,000 FWHM at 400 m/z. Up to the 10 most abundant peptides (minimum intensity of 500 counts) were selected from each MS scan and then fragmented using CID (collision-induced dissociation) in the linear ion trap using helium as collision gas with 38% normalized collision energy. The scan time settings were: full MS at 250ms and MSn at 120ms. Generated .raw data files were collected with Thermo Xcalibur (v.2.2) (Termo Fisher Scientific).

Proteomic Data Analysis

Raw data processing and database search

Proteome Discoverer software suite (v2.0, Thermo Fisher Scientific) and the Mascot search engine (v2.5, Matrix Science) were used for peptide identification and quantification. Samples were searched against a SwissProt database containing entries corresponding to Human (version of March 2018) a list of common contaminants and all the corresponding decoy entries. Trypsin was chosen as enzyme and a maximum of three miscleavages were allowed. Carbamidomethylation (C) was set as a fixed modification, whereas oxidation (M) and acetylation (N-terminal) were used as variable modifications. Searches were performed using a peptide tolerance of 7 ppm and a product ion tolerance of 0.5 Da. Resulting data files were filtered for FDR <1%. The raw data as well as the processed files were uploaded to the PRIDE repository with the project accession code PXD016261.

Bioinformatic analysis

The handling of the protein lists created with Proteome Discoverer as well as the generation of the Venn diagrams and bar plots were performed with R (3.5.2) and R Studio (1.1.419) with the help of the “Vennerable” package.

Gene Ontology enrichment analysis

The Gene Ontology enrichment analysis was performed with the DAVID Bioinformatics tools[9] (https://david.ncifcrf.gov/) using the “Functional Annotation” functionality. For this analysis, all the levels of specificity of the “Cellular Compartment” Ontology were selected (GOTERM_CC_ALL) and the “Functional Annotation Clustering” option was chosen for the visualization of the results. The enrichment threshold or statistical

significance (EASE score) was set to 0.001. The enriched GO terms related to the different cell compartments were extracted using R (3.5.2) and R Studio (1.1.419).

RESULTS AND DISCUSSION

TIF sample processing by centrifugation.

The amount of tissue is typically limited for the surplus biopsies of cSCC (0.1-0.3 gr). In this work, we split each tumor sample into two halves of about 0.1 gr and used each one in a different procedure of TIF extraction. First, we set up centrifugation method[10-11]. Key steps in this method were centrifugation parameters like G-forces and time of centrifugation. Excessive G-forces and time could cause the rupture of cells and hence the contamination of interstitial fluid with intracellular proteins. Certainly, these parameters had to be considered taking into account the particular characteristics of each tissue. In our hands, we needed high G-forces to obtain TIF from cSCC samples. Below 800 g, the volume recovered was always less than 1 µl. At 800 g for 20 minutes, the volume of the sample was less than 5 µl depending on the sample size. We got satisfactory volumes in all samples (5 to 15 µl) after spinning at 10.000 g for 20 minutes. All the samples were diluted with PBS containing protease inhibitors (iPBS) to a final volume of 50 µl with a protein concentration ranging from 5 to 30 mg/ml.

We compared the protein profiles obtained at 800 g and 10000 g from one tumor sample (SCC19). Both procedures showed similar profiles enriched in low molecular weight proteins when compared to plasma (Figure 1A-1B). To visualize the influence of G-force on proteome composition, two tumor samples (SCC18 and SCC19) each of them centrifuged at low and high revolutions (four samples in total) were analyzed by mass spectrometry. The Venn diagrams show the overlap of the identified proteins from the two spin conditions (Figure 2A-2B). The 90% of the proteins identified at 800 g were also found at 10000 g indicating that high G-force did not imply a loss of information. To analyze the variability among methods and samples, we calculated the Pearson correlation coefficient (PCC) of the mass spectrometry results. The heat map of PCC showed that the secretomes of different samples had a larger variation than the ones from distinct centrifugation conditions (Figure 2C), meaning that the biological variability clearly exceeded the technical variability.

Finally, we considered the risk of cell breakage in the 10000 g samples. In the samples SCC18 and SCC19, there were 136 and 122 proteins only identified at 800 g, whereas at 10000 g there were 292 and 362 not overlapped proteins, respectively (Figure 2A - 2B). We determined the percentage of GO terms related to subcellular localization of those non-common proteins (Figure 2D). We did not detect any significant bias at the

level of nuclear and membrane proteins in the samples obtained at 10000 g that would have pointed towards an increased cell breakage at higher centrifugation speed.
Additionally, we performed a semi-quantitative analysis of ribosomal proteins (based on the signal of 78 ribosomal proteins) using the PSMs detected in both extraction methods (elution and spin at 10000 g) which also show no statistical differences (Supplementary Table 2) indicating that the cell breakage is similar regardless of the methodology used. The list of ribosomal proteins included in the analysis are listed in Supplementary Table 3).

In order to determine spin method and LC-MS/MS analysis variability, we have performed technical replicates. The same tumor sample was split in two halves (SPIN1 and SPIN2) and each of them were processed for TIF extraction with the same spin protocol (10000 g; 20 min). The whole proteome obtained from SPIN2 sample was injected three times for LC-MS/MS analysis. The LC-MS/MS replicates showed 96-97% overlap suggesting a very good reproducibility (Suppl. Figure S1). Moreover, there is a high overlap (more than 95%) among the single technical replicate injected for SPIN1 and each of the three replicates injected for SPIN2 (Suppl. Figure S2).

Overall, these results indicate that the increment of G-force necessary to obtain TIF in samples of cSCC results in the identification of more proteins but it seems that does not trigger a strong generalized cell breakage, compared to lower G-forces or elution method. The requirement of this high G-force could be explained because the human skin is a very collagen-rich tissue, and the collagen alone accounts for approximately 75% of the dry weight of skin[12], providing it with a high tensile strength not present in other tissues.

Comparison of the proteomes generated by elution and spin methods

To obtain TIF samples by elution, we essentially used the procedure published by Celis *et al* [13]. In this method, the protein composition of the fluid depends on the diffusion of the proteins from the interstitium to the PBS. Since the interstitium of the skin is very rich in collagen and therefore quite dense[13], we incubated the tissue for two hours instead of one to extend the diffusion time in iPBS. Also, we incubated pieces of about 0.1 gr avoiding cutting tissue and thus reducing cell break. For all the samples, we recovered 500 µl of final volume with a protein concentration that ranged from 3 to 10 mg/ml. We tested the quality of the samples by SDS-PAGE and coomassie blue staining (Figure 1C - 1D). The protein profile of the cSCC sample substantially differed from plasma profile,

and was enriched mainly with low molecular weight proteins (below albumin) independently of the method used.

To compare elution and centrifugation (10000 g) methods, three tumor samples (SCC6, SCC8 and SCC9) each of them eluted and centrifuged (six samples in total) were analyzed by mass spectrometry. The total number of proteins identified was 2767 proteins by the elution method and 2869 by the spin method. The 88-89% of the proteins identified by spin and elution methods are found in extracellular vesicles (Vesiclepedia database, last version[15]) supporting TIF samples quality (Suppl. Figure S3; Suppl. Tables S4 and S5). The observed mean proteins intensities in every sample of spin method were significantly higher than the ones observed by elution method (Figure 3A). As a loading control, we have compared the PSMs found for some of the most abundant plasma proteins (Suppl. Table 1). As observed, none of the PSMs comparisons are statistically significant (rows 2 to 5) suggesting that the amounts of the most abundant proteins detected in both methods are indistinguishable. However, the comparison of the mean intensities (row 1) of both methods shows differences which are statistically significant ($p<0.005$). This would indicate that although the amount of proteins/peptides analyzed in every sample is similar the method B seems to improve the detection of proteins as observed in comparing the mean intensities.

Considering sample variability, only around 50% of proteins (52.7% and 52.6% in elution and spin method, respectively) were identified in all the three samples analyzed with the same method (Figure 3B - 3C). Multiple previous studies showed similar results: analyzing different biological samples of one tumor type other authors also found 50% of common proteins among samples[15-16]. The biological samples variability between different patients could be explained for multiple reasons, foremost tumor heterogeneity and characteristics of the patient. Our three patients were diagnosed of primary high risk cSCC with similar clinical and pathological characteristics, but each tumor may differ in their individual genetic and therefore also proteomic profile. All tumors were sampled from a chronically photoexposed area, but not exactly the same area: the face (SCC6), the wrist (SCC8) and the scalp (SCC9) (Table 1).

Regarding methods, the overlap among the total proteins obtained from the three samples in each method was 80.01% of proteins found by elution method and 77.17% of total proteins found by spin method (Figure 3D). The Pearson correlation coefficients indicate that the proteomes of different samples showed higher variability than the proteomes of different methods (Figure 3E). This result suggests that the methodology used in TIF extraction, centrifugation versus elution, does not strongly influence the proteomic profile of cSCC biopsies when comparing the same sample. However, a

relatively important number of proteins (553 of eluted proteins and 655 of spin-obtained proteins) were specific for each individual method. We analyzed the subcellular localization of method-specific proteins by using GO ontology classification (Figure 3F). The GO terms related to “nuclear” and “membrane” localizations were considerably increased (more than 10-fold and 6-fold increase, respectively) in the elution method whereas the “extracellular” localization was enriched in the spin method (around 3-fold increase). This last result suggests that centrifugation is the suitable method to obtain TIF samples from cSCC.

To our knowledge this is the first study comparing the methodologies used to obtain TIF in samples of the same patient and tumor. We have checked in the literature for dataset of TIF of the same kind of tumor processed with elution or centrifugation. For instance, the proteomic analysis of TIF of ovarian carcinoma obtained by Hoskins *et al*[16] using elution and by Haslene-Hox *et al*[11] using centrifugation. In these studies, 569 total proteins were obtained using elution and 769 using centrifugation and 284 of the proteins were common to both methods. This means an overlap of 50% in elution and 37% in centrifugation. Although these studies are not directly comparable with our results, the number of proteins obtained with centrifugation method is also higher. Moreover, considering the differences among patients, tumors and mass spectrometry set up, the overlap achieved with the TIF data of ovarian cancer in these independent studies seems relevant.

CONCLUSIONS

In this paper, we suggest a “workflow” to set up TIF isolation in tumor tissues that includes the comparison of different methods with pieces of the same tumor. Protocol characteristics may be set up for each tumor. The choice of a method rather depends on the consistency and the handling of the tissue, than on method quality as such. We propose that centrifugation is the method of choice to obtain TIF in cSCC biopsies. We got more extracellular proteins, greater sensitivity and easier and quicker handling of samples. The spin method is very well adjustable to the mean size of the cSCC biopsies. The main concern associated to the centrifugation method is cell breaking during the spin of the biopsy at high G-forces[10-11]. However, our data indicate that the level of cell integrity after spin (10000 g) or after elution may be very similar because the proteome profile was quite conserved. Moreover, centrifuged samples showed low levels of nuclear and membrane proteins and enrichment in extracellular proteins. Then, these data suggest that during centrifugation the cell lysis is not elevated.

The authors declare no competing financial interest.

ACKNOWLEDGEMENTS AND FUNDINGS

We thank Rosa Ayala for analyzing already published TIF dataset and the members of the dermatology department of HUAV to collaborate for the sample collection. This work was funded by Catalan Government (2017-SGR-569). C Matas is recipient of an intramural grant from Lleida Institute for Biomedical Research-Dr. Pifarré Foundation supported by Diputació de Lleida. M. Guasch was supported by a predoctoral fellowship from UdL. The proteomics analyses were performed in the IDIBELL Clinical Proteomic unit that is part of the Proteored, PRB3 and is supported by grant PT17/0019, of the PE I+D+i 2013-2016, funded by ISCIII and ERDF. This article is dedicated to Glòria Nadal Xifra and Narcís Matas Ros.

REFERENCES

1. Karagiannis GS, Pavlou MP, Diamandis EP. Cancer secretomics reveal pathophysiological pathways in cancer molecular oncology. Mol Oncol. **2010**; 4:496-510.
2. Gullino PM, Clark SH, Grantham FH. The interstitial fluid of solid tumors. Cancer Res. **1964** ;24:780-94.
3. Wagner M., Wiig H. Tumor Interstitial Fluid Formation, Characterization and Clinical Implications. Front Oncol. **2015**; 5:1-12.
4. Onsurathum S, Haonon O, Pinlaor P, Pairojkul C, Khuntikeo N, Thanan R, Roytrakul S, Pinlaor S. Proteomics detection of S100A6 in tumor tissue interstitial fluid and evaluation of its potential as a biomarker of cholangiocarcinoma. Tumour Biol. **2018**; 40:1010428318767195.
5. Chen EI, Yates JR 3rd. Cancer proteomics by quantitative shotgun proteomics. Mol Oncol. **2007**, 1,144-159.
6. Bittremieux W, Tabb DL, Impens F, Staes A, Timmerman E, Martens L, Laukens K. Quality control in mass spectrometry-based proteomics. Mass Spectrom Rev. **2018**; 37:697-711.
7. Bodzon-Kulakowska A, Bierczynska-Krzysik A, Dylag T, Drabik A, Suder P, Noga M, Jarzebinska J, Silberring J. Methods for samples preparation in proteomic research. J Chromatogr B Analyt Technol Biomed Life Sci. **2007**; 15; 849:1-31.

8. Haslene-Hox H. Measuring gradients in body fluids - A tool for elucidating physiological processes, diagnosis and treatment of disease. Clin Chim Acta. **2018**, 23. S0009-8981: 30423-6.

9. Huang DW, Sherman BT, Lempicki RA. Systemic and integrative analysis of large gene lists using DAVID bioinformatic resources. Nature Protocols 2009; 4:44.

10. Wiig H, Aukland K and Tenstad O. Isolation of interstitial fluid from rat mammary tumors by a centrifugation method. Am J Physiol Heart Circ Physiol. **2003**, 284: H416-H424.

11. Haslene-Hox H, Oveland E, Berg KC, Kolmannskog O, Woie K, Salvesen HB, Tenstad O and Wiig H. A new method for isolation of interstitial fluid from human solid tumors applied to proteomic analysis of ovarian carcinoma tissue. PLoS One 6*.* **2011***,* e192-117.

12. David H. Chu. Development and structure of skin. *In Fitzpatrick's Dermatology in General Medicine*. 7th ed.; Mc Graw Hill Medical Ed, **2008**; p 63.

13. Celis JE, Gromov P, Cabezón T, Moreira JM, Ambartsumian N, Sandelin K, Rank F, Gromova I. Proteomic characterization of the interstitial fluid perfusing the breast tumor microenvironment: a novel resource for biomarker and therapeutic target discovery. Mol Cell Proteomics. **2004**, 3, 327-344.

14. Holliday MA. Extracellular fluid and its proteins: dehydration, shock, and recovery. Pediatr Nephrol. **1999**; 13:989-95.

15. R.J. Fijneman, M. de Wit, M. Pourghiasian, S.R. Piersma, T.V. Pham, M.O. Warmoes, M. Lavaei, C. Piso, F. Smit, P.M. Delis-van Diemen, S.T. van Turenhout, J.S. Terhaar Sive Droste, C.J. Mulder, M.A. Blankenstein, E.C. Robanus-Maandag, R. Smits, R. Fodde, V.W. van Hinsbergh, G.A. Meijer, C.R. Jimenez. Proximal fluid proteome profiling of mouse colon tumors reveals biomarkers for early diagnosis of human colorectal cancer, Clin Cancer Res. **2012**, 18, 2613–2624.

16. Hoskins ER., Hood BL., Sun M., Krivak TC., Edwards RP., and Conrads TP. Proteomic analysis of ovarian càncer proximal fluids: Validation of elevated peroxiredoxin 1 in patient peripheral circulation. PLoS ONE. **2011**; 6,1-7.

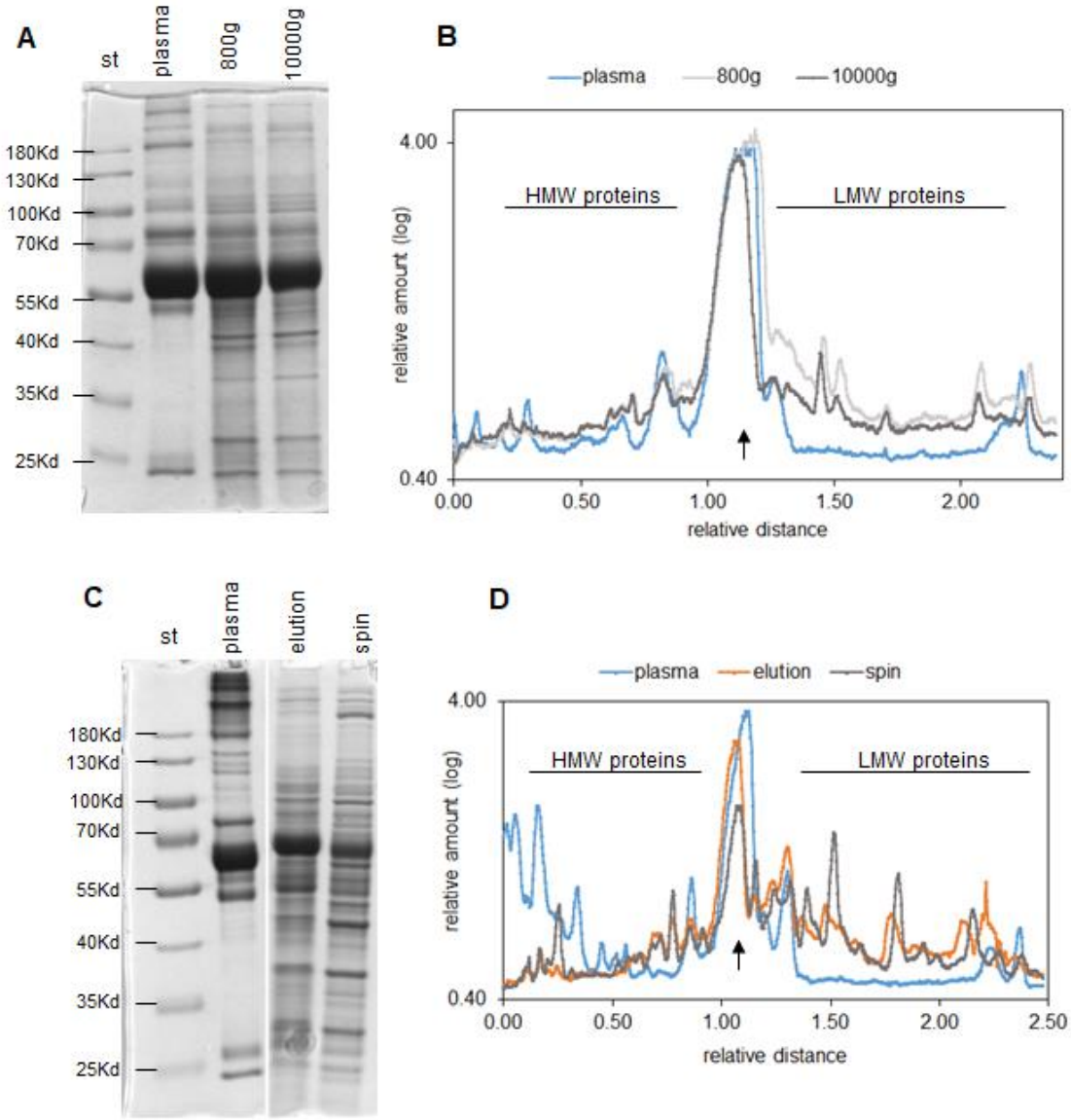

Figure 1. Sample processing. A) TIF samples of the same biopsy SCC19 obtained by spin at 800 g (5 µl) and at 10000 g (2.5 µl) were analyzed by SDS-PAGE in 10% polyacrylamide gel. Picture of the gel stained with Coomassie Blue. **B**) Protein profile obtained from A with the Image J program. **C)** TIF samples of the same biopsy SCC6 obtained by elution (7.5 µl) and by spin (5 µl) were analyzed by SDS-PAGE in 10% polyacrylamide gel. Picture of the gel stained with Coomassie Blue. **D)** Protein profile obtained from C with the Image J program.
A molecular weight standard (st) and plasma were also loaded in the gel as controls. High and Low Molecular Weight regions are indicated as HMW and LMW, respectively. Arrow indicates Albumin peak position.

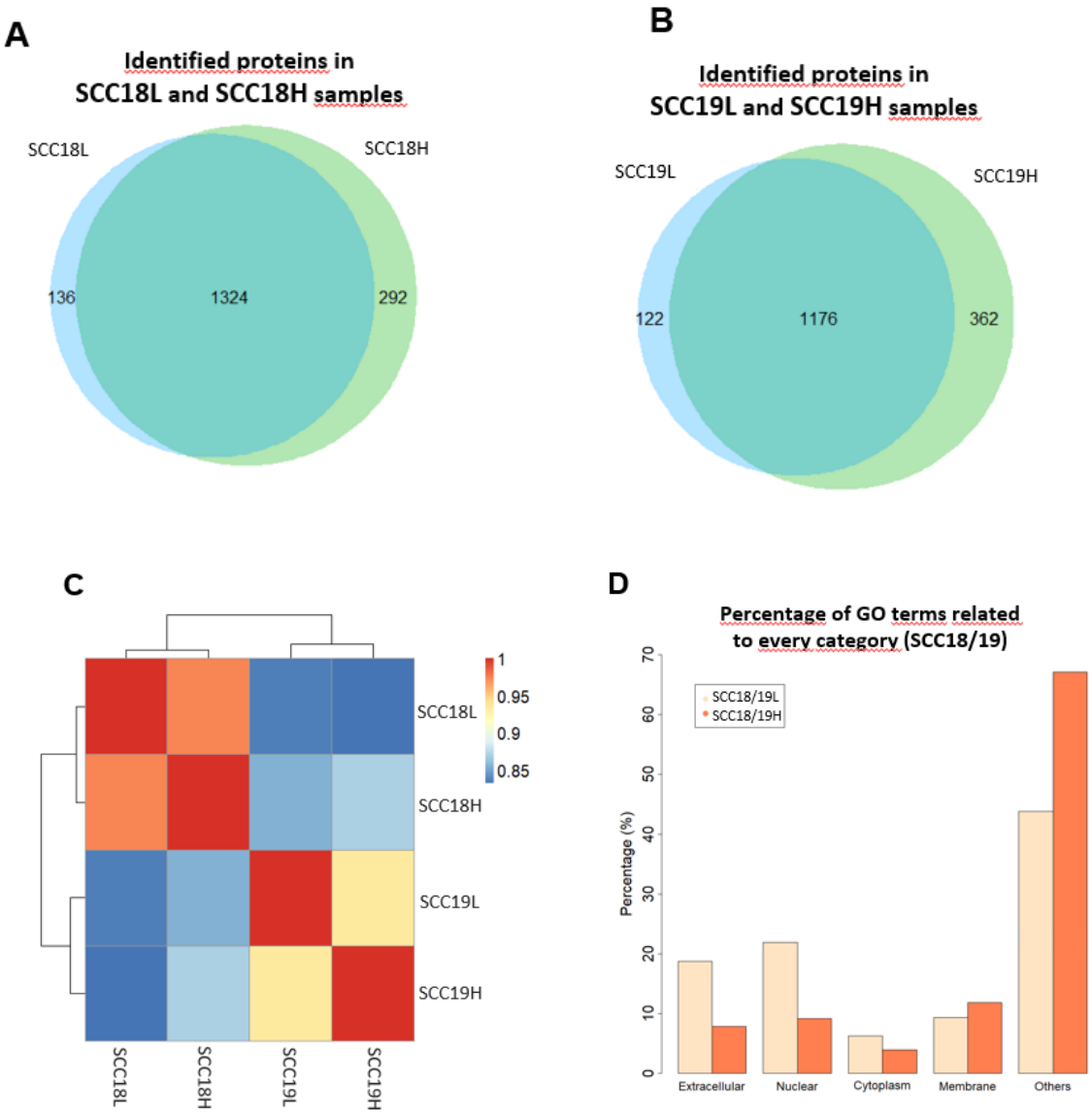

Figure 2. Characteristics of TIF samples obtained by centrifugation. A and B) Venn diagrams representing the overlap among the TIF proteins detected by centrifugation at 800 g (L) and at 10000 g (H). The numbers indicate identified proteins. **C)** Heat map of Pearson correlation coefficients comparing tumor samples and methods. **D)** Percentage distribution of GO terms related to subcellular categories. The graphic compares the non-overlapping proteins obtained by centrifugation at 800 g (L) and at 10000 g (H).

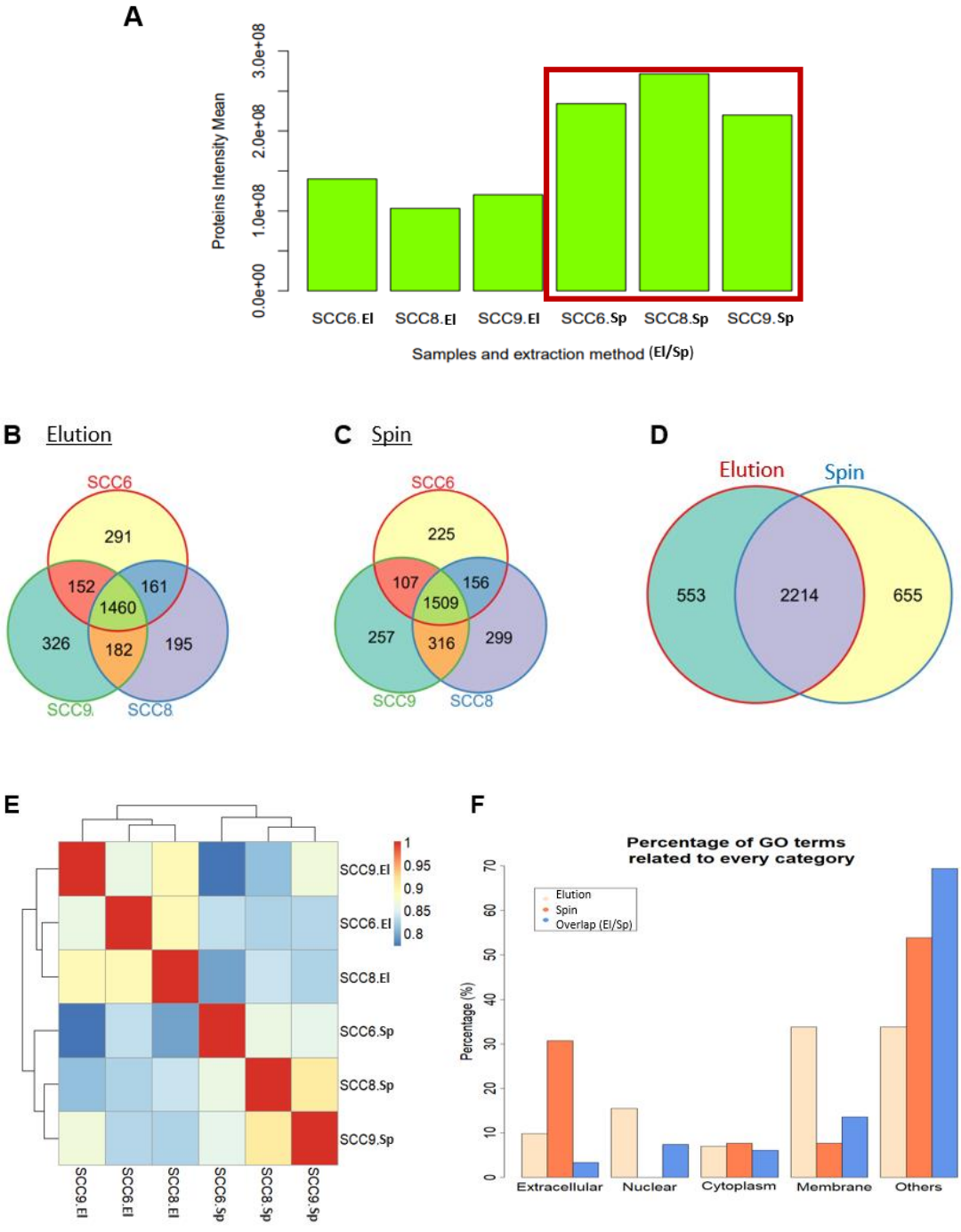

Figure 3. Comparison of the secretome obtained by elution and spin. **A)** Graphic representing the proteins intensity mean in each sample for both methods, elution (El) and spin (Sp). **B)** and **C)** Venn diagram representing the overlapping in the proteome of tumor samples obtained by elution (B) and spin (C). **D)** Venn diagrams representing the

overlap among the TIF proteins detected by elution and by spin. The numbers indicate identified proteins. **E)** Heat map of Pearson correlation coefficients comparing tumor samples and methods. **F)** Percentage distribution of GO terms related to subcellular categories. The graphic compares the non-overlapping proteins obtained by elution and by centrifugation.

Table 1. Patients and tumors characteristics from the 5 analyzed samples.

Sample	Gender	Age	Tumor localization	Tumor size	Tumor characteristics
SCC6	Male	90	Wrist	3 cm	Primary tumor
SCC8	Male	84	Scalp	2 cm	Primary tumor
SCC9	Male	80	Face (right cheek)	3’5 cm	Primary tumor
SCC18	Male	80	Face (left cheek)	4 cm	Primary tumor
SCC19	Female	64	Right Foot	3 cm	Primary tumor

SUPPLEMENTARY FILES

Supplementary table 1: Comparisons of the PSMs found in both methods (elution (left) and spin at 10000 g (right)) for Albumin (P02768), Serotransferrin (P02787), fibrinogen alpha chain precursor (P02671) and fibrinogen beta chain precursor (P02675). Showing the associated p-values to the Student t-tests applied to check the statistical significance.

	Replicate 1	Replicate 2	Replicate 3	Replicate 1	Replicate 2	Replicate 3	t test - p value (Method A vs Method B)
Mean Intensities	140028406	103131901	120162934	234155739	271482513	219936386	0.004377336
Albumin (P02768) PSMs	256	196	270	240	317	291	0.260096781
Serotransferrin (P02787) PSMs	50	39	73	56	60	69	0.534109047
Fibrinogen α chain (P02671) PSMs	36	33	36	30	42	38	0.688493788
Fibrinogen β chain (P02675) PSMs	27	32	33	33	41	33	0.207024705

Supplementary table 2: Semi-quantitative analysis of ribosomal proteins (based on the signal of 78 ribosomal proteins) using the PSMs detected in both extraction methods (elution and spin at 10000 g). Showing the associated p-values to the Student t-tests applied to check the statistical significance

	METHOD A			METHOD B			
	Replicate 1	Replicate 2	Replicate 3	Replicate 1	Replicate 2	Replicate 3	t test - p value (Method A vs Method B)
Ribosomal Proteins PSMs	261	229	289	222	316	368	0.434480967

Supplementary table 3: List of ribosomal proteins included in the analysis.

Accession	Protein Name
P39023	60S ribosomal protein L3 OS=Homo sapiens GN=RPL3 PE=1 SV=2
P26373	60S ribosomal protein L13 OS=Homo sapiens GN=RPL13 PE=1 SV=4
P05388	60S acidic ribosomal protein P0 OS=Homo sapiens GN=RPLP0 PE=1 SV=1
P30050	60S ribosomal protein L12 OS=Homo sapiens GN=RPL12 PE=1 SV=1
P08865	40S ribosomal protein SA OS=Homo sapiens GN=RPSA PE=1 SV=4
P50914	60S ribosomal protein L14 OS=Homo sapiens GN=RPL14 PE=1 SV=4
P63220	40S ribosomal protein S21 OS=Homo sapiens GN=RPS21 PE=1 SV=1
P39019	40S ribosomal protein S19 OS=Homo sapiens GN=RPS19 PE=1 SV=2
P62906	60S ribosomal protein L10a OS=Homo sapiens GN=RPL10A PE=1 SV=2
P61513	60S ribosomal protein L37a OS=Homo sapiens GN=RPL37A PE=1 SV=2
P46783	40S ribosomal protein S10 OS=Homo sapiens GN=RPS10 PE=1 SV=1
Q02878	60S ribosomal protein L6 OS=Homo sapiens GN=RPL6 PE=1 SV=3
P42766	60S ribosomal protein L35 OS=Homo sapiens GN=RPL35 PE=1 SV=2
P60866	40S ribosomal protein S20 OS=Homo sapiens GN=RPS20 PE=1 SV=1
P49207	60S ribosomal protein L34 OS=Homo sapiens GN=RPL34 PE=1 SV=3
P62273	40S ribosomal protein S29 OS=Homo sapiens GN=RPS29 PE=1 SV=2
P62277	40S ribosomal protein S13 OS=Homo sapiens GN=RPS13 PE=1 SV=2
Q9Y3U8	60S ribosomal protein L36 OS=Homo sapiens GN=RPL36 PE=1 SV=3
P62917	60S ribosomal protein L8 OS=Homo sapiens GN=RPL8 PE=1 SV=2
P62241	40S ribosomal protein S8 OS=Homo sapiens GN=RPS8 PE=1 SV=2
P18077	60S ribosomal protein L35a OS=Homo sapiens GN=RPL35A PE=1 SV=2
P62847	40S ribosomal protein S24 OS=Homo sapiens GN=RPS24 PE=1 SV=1
P62979	Ubiquitin-40S ribosomal protein S27a OS=Homo sapiens GN=RPS27A PE=1 SV=2
P36578	60S ribosomal protein L4 OS=Homo sapiens GN=RPL4 PE=1 SV=5
P05386	60S acidic ribosomal protein P1 OS=Homo sapiens GN=RPLP1 PE=1 SV=1
P62269	40S ribosomal protein S18 OS=Homo sapiens GN=RPS18 PE=1 SV=3
P62753	40S ribosomal protein S6 OS=Homo sapiens GN=RPS6 PE=1 SV=1
P27635	60S ribosomal protein L10 OS=Homo sapiens GN=RPL10 PE=1 SV=4
P62841	40S ribosomal protein S15 OS=Homo sapiens GN=RPS15 PE=1 SV=2
P62829	60S ribosomal protein L23 OS=Homo sapiens GN=RPL23 PE=1 SV=1
P84098	60S ribosomal protein L19 OS=Homo sapiens GN=RPL19 PE=1 SV=1
P62280	40S ribosomal protein S11 OS=Homo sapiens GN=RPS11 PE=1 SV=3
Q02543	60S ribosomal protein L18a OS=Homo sapiens GN=RPL18A PE=1 SV=2
P42677	40S ribosomal protein S27 OS=Homo sapiens GN=RPS27 PE=1 SV=3
P40429	60S ribosomal protein L13a OS=Homo sapiens GN=RPL13A PE=1 SV=2
P62899	60S ribosomal protein L31 OS=Homo sapiens GN=RPL31 PE=1 SV=1
P61927	60S ribosomal protein L37 OS=Homo sapiens GN=RPL37 PE=1 SV=2
P32969	60S ribosomal protein L9 OS=Homo sapiens GN=RPL9 PE=1 SV=1
P46779	60S ribosomal protein L28 OS=Homo sapiens GN=RPL28 PE=1 SV=3
Q07020	60S ribosomal protein L18 OS=Homo sapiens GN=RPL18 PE=1 SV=2
P62861	40S ribosomal protein S30 OS=Homo sapiens GN=FAU PE=1 SV=1
P62081	40S ribosomal protein S7 OS=Homo sapiens GN=RPS7 PE=1 SV=1
P23396	40S ribosomal protein S3 OS=Homo sapiens GN=RPS3 PE=1 SV=2
Q9BYN8	28S ribosomal protein S26, mitochondrial OS=Homo sapiens GN=MRPS26 PE=1 SV=1
P62913	60S ribosomal protein L11 OS=Homo sapiens GN=RPL11 PE=1 SV=2
P62266	40S ribosomal protein S23 OS=Homo sapiens GN=RPS23 PE=1 SV=3
P63173	60S ribosomal protein L38 OS=Homo sapiens GN=RPL38 PE=1 SV=2
P61353	60S ribosomal protein L27 OS=Homo sapiens GN=RPL27 PE=1 SV=2
P62424	60S ribosomal protein L7a OS=Homo sapiens GN=RPL7A PE=1 SV=2
P62888	60S ribosomal protein L30 OS=Homo sapiens GN=RPL30 PE=1 SV=2
P18621	60S ribosomal protein L17 OS=Homo sapiens GN=RPL17 PE=1 SV=3
P62910	60S ribosomal protein L32 OS=Homo sapiens GN=RPL32 PE=1 SV=2
P46778	60S ribosomal protein L21 OS=Homo sapiens GN=RPL21 PE=1 SV=2
P35268	60S ribosomal protein L22 OS=Homo sapiens GN=RPL22 PE=1 SV=2
P46777	60S ribosomal protein L5 OS=Homo sapiens GN=RPL5 PE=1 SV=3
P62701	40S ribosomal protein S4, X isoform OS=Homo sapiens GN=RPS4X PE=1 SV=2
P62263	40S ribosomal protein S14 OS=Homo sapiens GN=RPS14 PE=1 SV=3
P62851	40S ribosomal protein S25 OS=Homo sapiens GN=RPS25 PE=1 SV=1
P83731	60S ribosomal protein L24 OS=Homo sapiens GN=RPL24 PE=1 SV=1
P62854	40S ribosomal protein S26 OS=Homo sapiens GN=RPS26 PE=1 SV=3
P15880	40S ribosomal protein S2 OS=Homo sapiens GN=RPS2 PE=1 SV=2
P61247	40S ribosomal protein S3a OS=Homo sapiens GN=RPS3A PE=1 SV=2
P61254	60S ribosomal protein L26 OS=Homo sapiens GN=RPL26 PE=1 SV=1
P46782	40S ribosomal protein S5 OS=Homo sapiens GN=RPS5 PE=1 SV=4
P46781	40S ribosomal protein S9 OS=Homo sapiens GN=RPS9 PE=1 SV=3
P61313	60S ribosomal protein L15 OS=Homo sapiens GN=RPL15 PE=1 SV=2
P18124	60S ribosomal protein L7 OS=Homo sapiens GN=RPL7 PE=1 SV=1
P62750	60S ribosomal protein L23a OS=Homo sapiens GN=RPL23A PE=1 SV=1
P25398	40S ribosomal protein S12 OS=Homo sapiens GN=RPS12 PE=1 SV=3
P83881	60S ribosomal protein L36a OS=Homo sapiens GN=RPL36A PE=1 SV=2
P62244	40S ribosomal protein S15a OS=Homo sapiens GN=RPS15A PE=1 SV=2
P08708	40S ribosomal protein S17 OS=Homo sapiens GN=RPS17 PE=1 SV=2
P05387	60S acidic ribosomal protein P2 OS=Homo sapiens GN=RPLP2 PE=1 SV=1
P62249	40S ribosomal protein S16 OS=Homo sapiens GN=RPS16 PE=1 SV=2
P62857	40S ribosomal protein S28 OS=Homo sapiens GN=RPS28 PE=1 SV=1
P46776	60S ribosomal protein L27a OS=Homo sapiens GN=RPL27A PE=1 SV=2
P47914	60S ribosomal protein L29 OS=Homo sapiens GN=RPL29 PE=1 SV=2
Q9HD33	39S ribosomal protein L47, mitochondrial OS=Homo sapiens GN=MRPL47 PE=1 SV=2